
Article:
Pabois, O orcid.org/0000-0001-5307-7149, Lorenz, CD, Harvey, RD et al. (5 more authors) (2019) Molecular insights into the behaviour of bile salts at interfaces: a key to their role in lipid digestion. Journal of Colloid and Interface Science, 556. pp. 266-277. ISSN 0021-9797

https://doi.org/10.1016/j.jcis.2019.08.010

Molecular insights into the behaviour of bile salts at interfaces: a key to their role in lipid digestion

Olivia Pabois[a, b], Christian D. Lorenz[c], Richard D. Harvey[d], Isabelle Grillo[a], Myriam M.-L. Grundy[e], Peter J. Wilde[f], Yuri Gerelli[a*], Cécile A. Dreiss[b*]

[a] Institut Laue-Langevin, Grenoble 38000, France

[b] Institute of Pharmaceutical Science, King's College London, London SE1 9NH, United-Kingdom

[c] Department of Physics, King's College London, London WC2R 2LS, United-Kingdom

[d] Institut für Pharmazie, Martin-Luther-Universität Halle-Wittenberg, Halle (Saale) 06099, Germany

[e] School of Agriculture, Policy and Development, University of Reading, Reading RG6 6AR, United-Kingdom

[f] Quadram Institute Bioscience, Norwich Research Park, Norwich NR4 7UA, United-Kingdom

E-mail addresses:

olivia.pabois@kcl.ac.uk; chris.lorenz@kcl.ac.uk; richard.harvey@pharmazie.uni-halle.de; grillo@ill.fr; m.m.grundy@reading.ac.uk; peter.wilde@quadram.ac.uk; gerelli@ill.fr; cecile.dreiss@kcl.ac.uk

Corresponding authors:

Cécile A. Dreiss:

King's College London
Institute of Pharmaceutical Science
Franklin-Wilkins Building
150 Stamford Street
SE1 9NH London, UK
Tel: +44 (0)207 848 3766

Yuri Gerelli:

Institut Max von Laue - Paul Langevin

71 avenue des Martyrs
38000 Grenoble, France
Tel: +33 (0)4 76 20 70 68

Supporting information

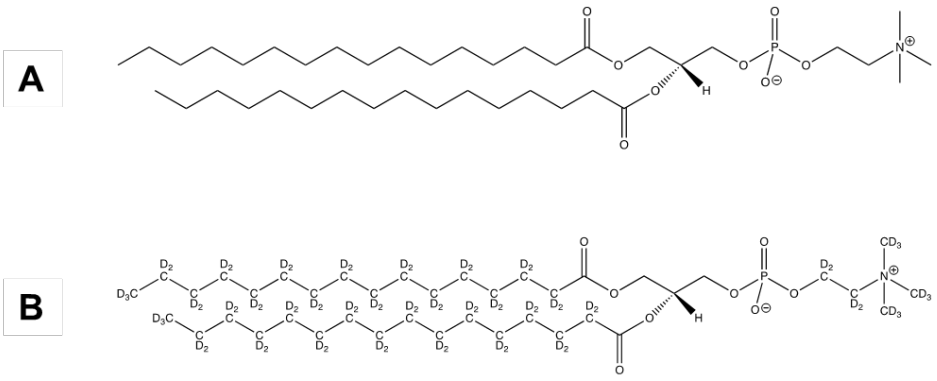

Figure S1: Structures of DPPC (A) and d_{75}-DPPC (B)

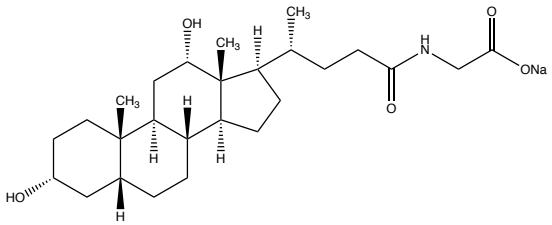

Figure S2: Structure of NaGDC

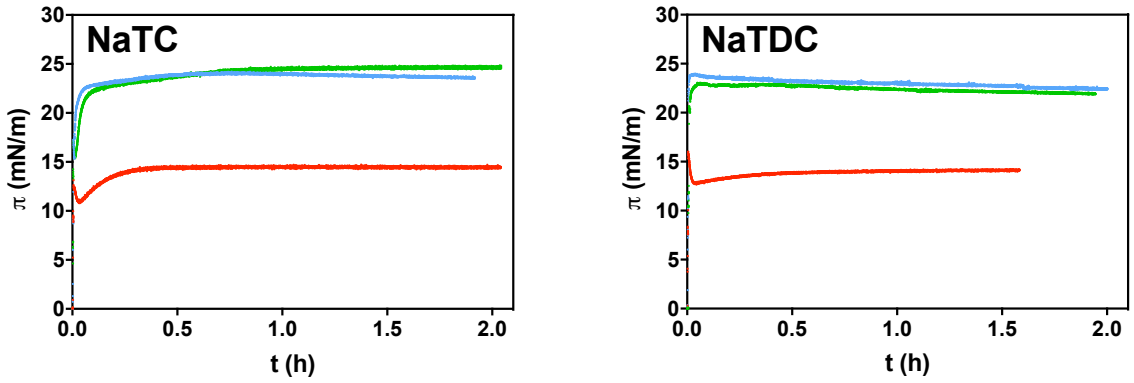

Figure S3: Time-dependent evolution of the surface pressure (π) measured by a LT, upon injection of BS into the aqueous subphase: NaTC, NaTDC, at varying concentrations: (—) 0.5 mM, (—) 5 mM, (—) 10 mM (at 23 ± 2°C). Each experiment was reproduced twice, and the average measurement was selected for each BS at each concentration.

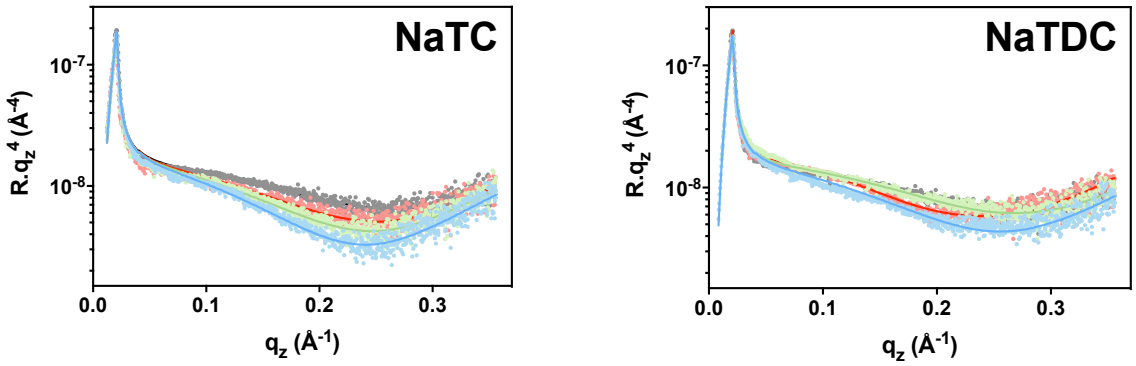

Figure S4: XRR signal ($R.q_z^4$ representation) of ultrapure water (●) and of the interfacial film formed at the air/water interface upon successive injections of BS into the aqueous subphase: NaTC, NaTDC (at 23 ± 2°C), as a function of the scattering vector (q_z). BS concentrations below ((●) 1 mM), around ((●) 5 mM), and above ((●) 10 mM) their CMC were selected because different interfacial behaviours were observed with the LT.

NaTC	Water	[NaTC] (mM)		
		1	5	10
σ (Å)	4	5	6	6
t (Å)	-	-	-	-
Electron density (×10^6) (Å^{-2})	-	-	-	-

NaTDC	Water	[NaTDC] (mM)		
		1	5	10
σ (Å)	4	5	4	5
t (Å)	-	33	24	-
Electron density (×10^6) (Å^{-2})	-	9.7	9.6	-

Table S1: Evolution of the XRR parameters of the interfacial film formed at the air/water interface upon successive injections of 1, 5 and 10 mM BS into the aqueous subphase: NaTC, NaTDC. When the layer formed was very diffuse, the evolution of the air/water interfacial roughness (σ) was monitored, while a model assuming a single layer characterised by a specific roughness (σ), thickness (t), and electron density, was used to fit a more dense, well-defined film.

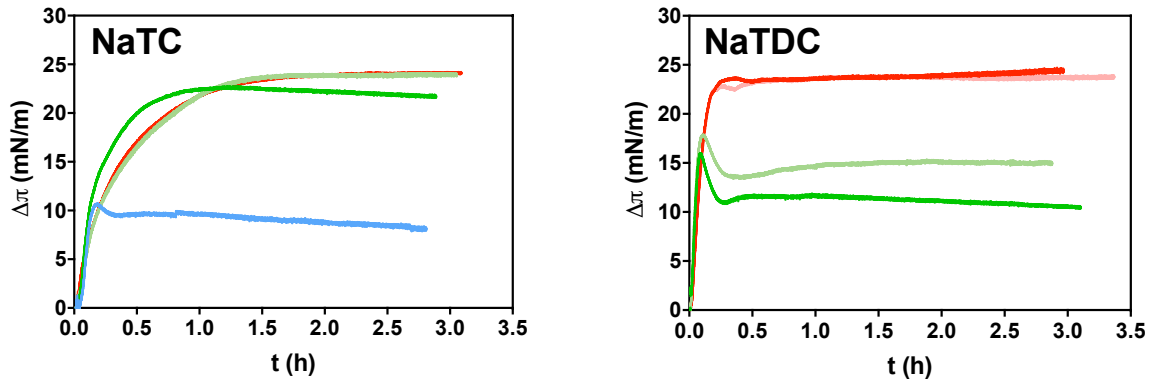

Figure S5: Time-dependent evolution of the surface pressure ($\Delta\pi(t) = \pi(t) - \pi_{DPPC}$) measured by a LT, upon injection of BS into the aqueous subphase: NaTC, NaTDC, at varying concentrations: (—) 0.5 mM, (—) 1 mM, (—) 5 mM, (—) 10 mM, (—) 20 mM (at 23 ± 2°C). The lipids were spread onto water at π_{DPPC} = 25 ± 2 mN/m. Each experiment was reproduced twice, and the average measurement was selected for each BS at each concentration.

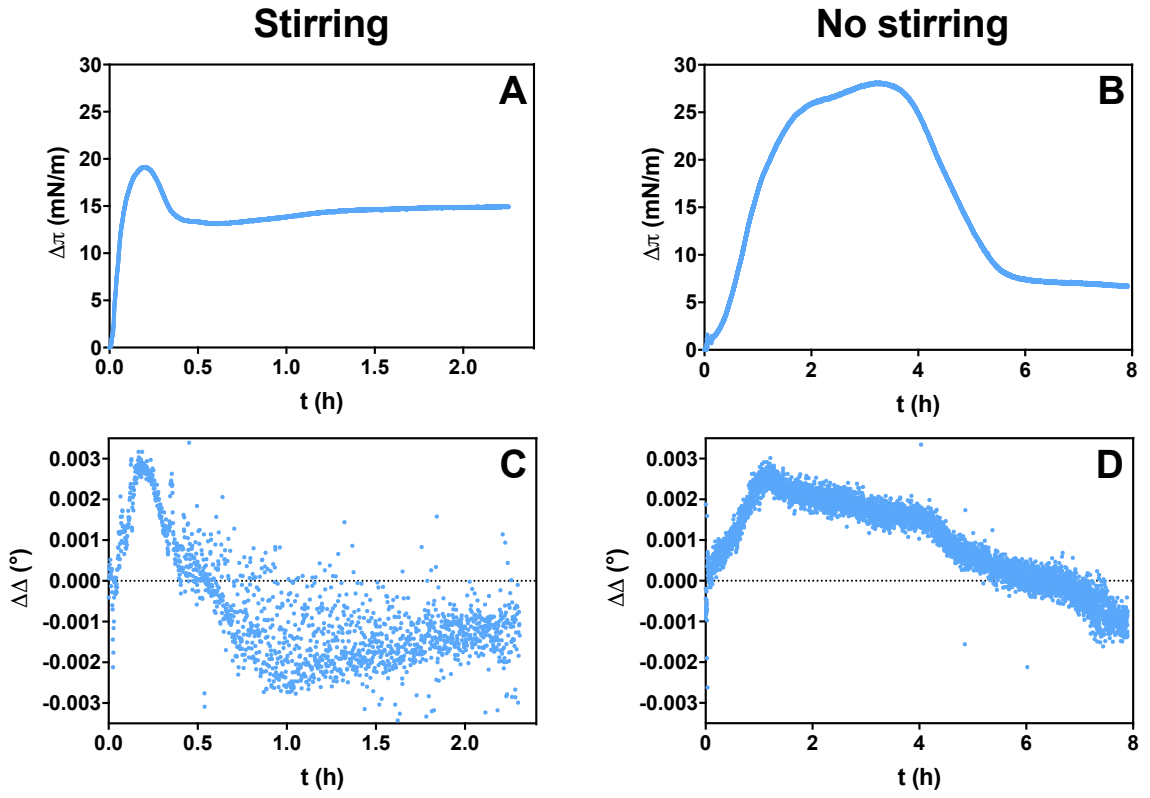

Figure S6: Time-dependent evolution of the surface pressure ($\Delta\pi(t) = \pi(t) - \pi_{DPPC}$) measured by a LT (A, B), and phase shift ($\Delta\Delta(t) = \Delta(t) - \Delta_{DPPC}$) measured by ellipsometry (C, D), upon addition of 10 mM NaTDC into the aqueous subphase, in the presence (A, C) and absence (B, D) of stirring (at 23 ± 2°C). The lipids were spread onto water at π_{DPPC} = 25 ± 2 mN/m, reaching Δ_{DPPC} = 3.20 °.

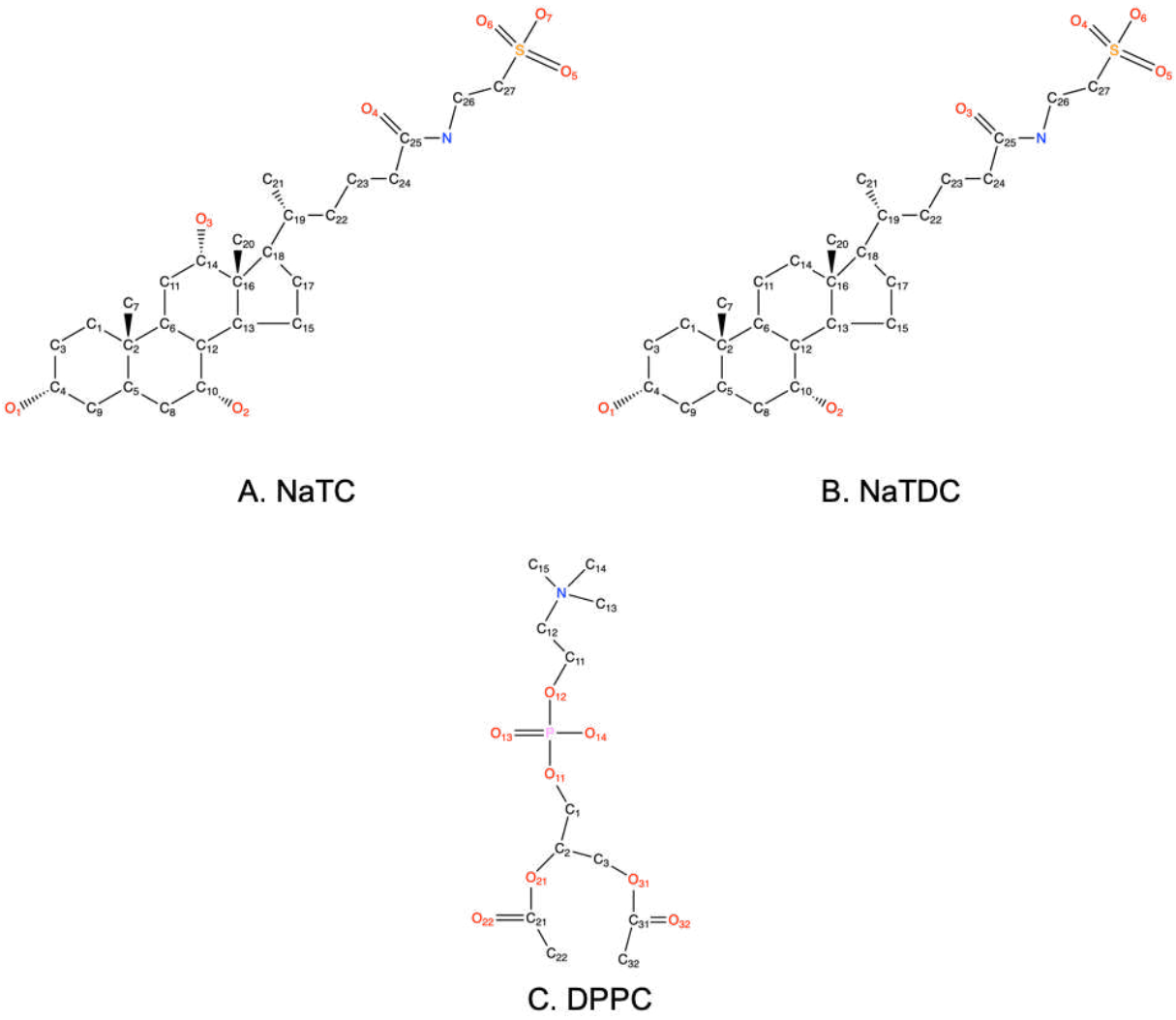

Figure S7: Definition of the atoms labels used in the interaction maps between molecules: A. NaTC, B. NaTDC, C. DPPC.

In order to characterise the interactions between the BS and DPPC monolayers, we have determined the interaction maps between the two molecules. In order to present these in a tractable manner, atom names were used in the manuscript for the heavy atoms in each BS and within the head group portion of the DPPC molecule. In Figure S7, we show the definition of these atom labels in terms of the chemical structure of each molecule.

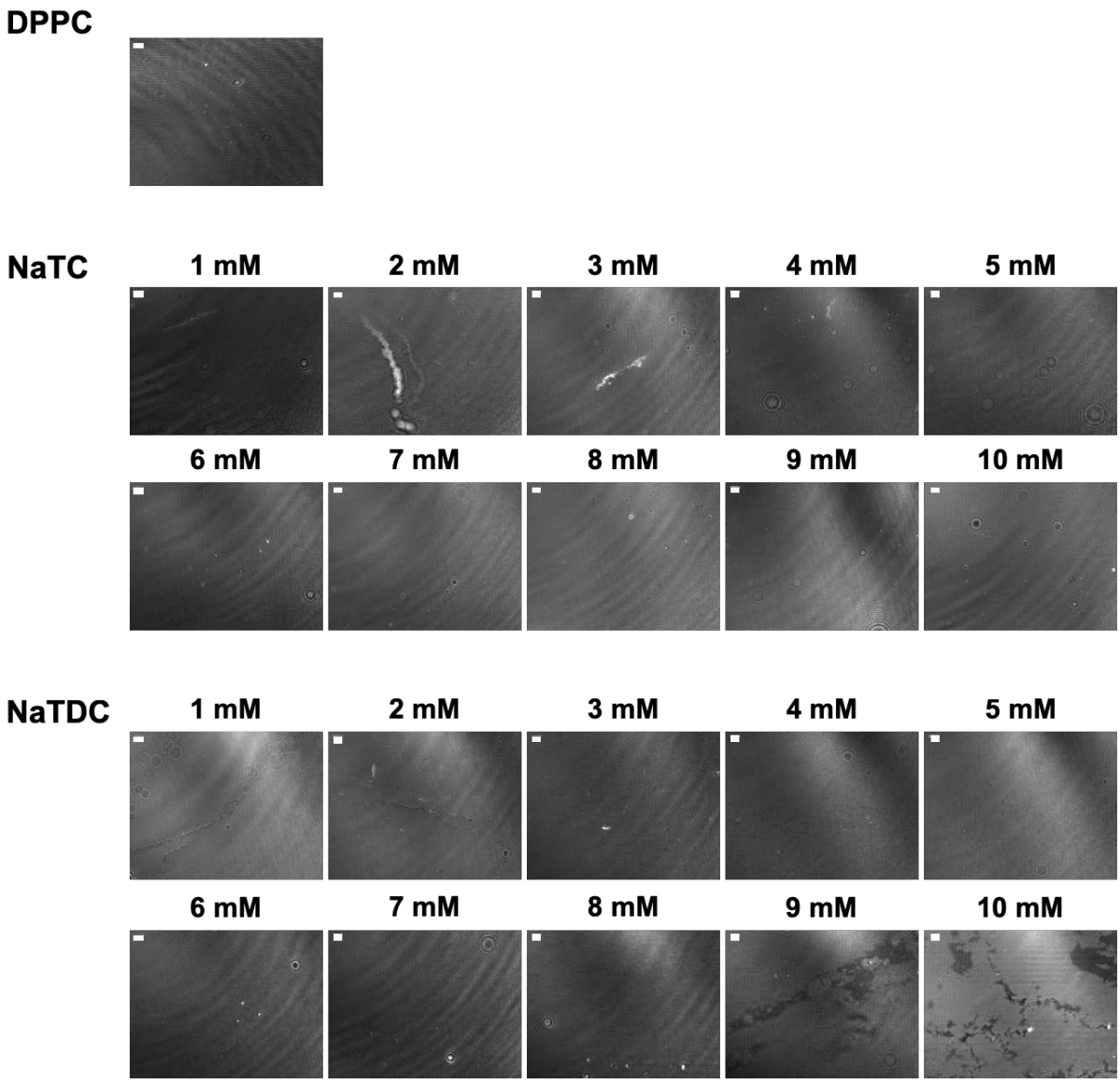

Figure S8: Evolution of the lipid monolayer organisation observed with a Brewster angle microscope, upon successive injections of BS into the aqueous subphase: NaTC, NaTDC (at 23 ± 2°C). The lipids were spread onto water at π_{DPPC} = 25 ± 2 mN/m. The scale bar of the BAM images is 50 µm. Stripes are caused by stirring-induced vibrations of the water subphase and (black or white) circular shapes are due to dust grains.

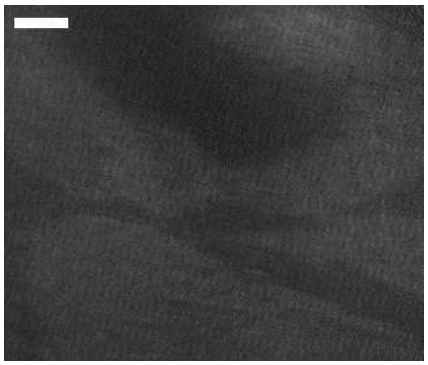

Figure S9: Evolution of the lipid monolayer organisation observed with a Brewster angle microscope, upon addition of 10 mM NaTDC into the aqueous subphase, under stirring (at 23 ± 2°C). The lipids were spread onto water at π_{DPPC} = 25 ± 2 mN/m. The scale bar of the BAM images is 50 µm.

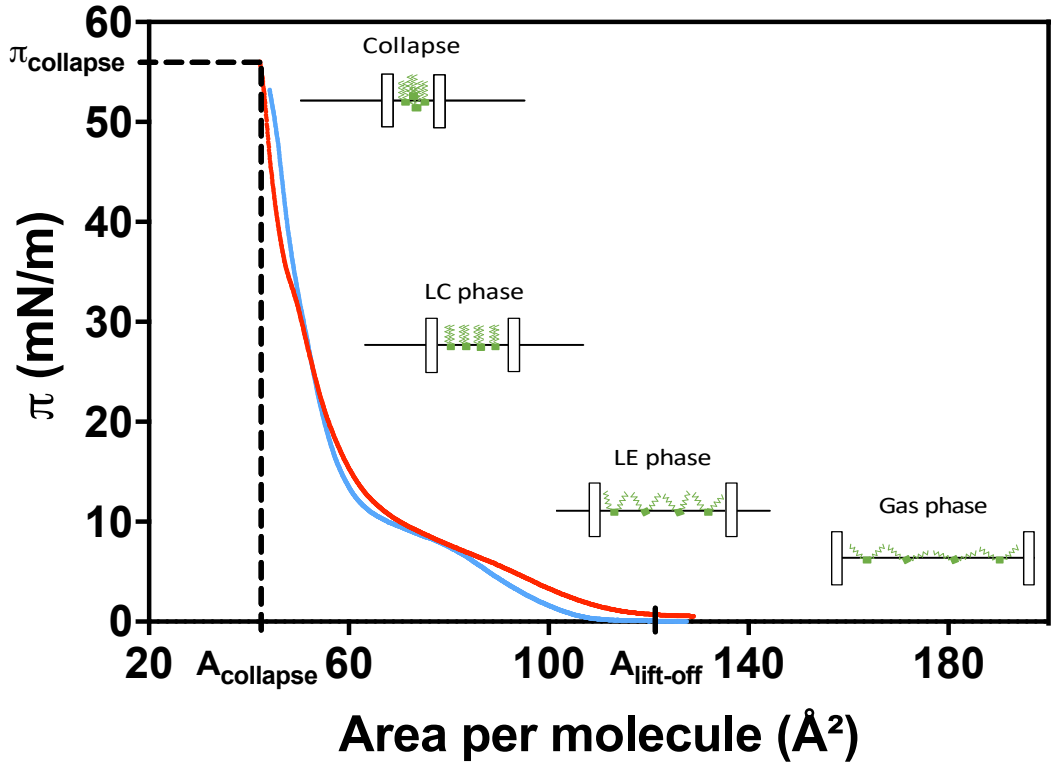

Figure S10: DPPC (—) and d_{75}-DPPC (—) π – A Langmuir isotherms. The phospholipids were deposited onto ultrapure water, at a low concentration (gas phase), and compressed (at 23 ± 2°C). $A_{lift\text{-}off}$ corresponds to the minimal surface density at which molecules start interacting and enter into the liquid-expanded (LE) state. Upon further compression, the sharper increase in surface pressure indicates the onset of a much more ordered and packed liquid-condensed (LC) monolayer. $A_{collapse}$ and $\pi_{collapse}$ are, respectively, the mean molecular area and surface pressure at which the film breaks. The different monolayer phases and related molecular organisations observed in the different regions of the isotherm are depicted in the figure.

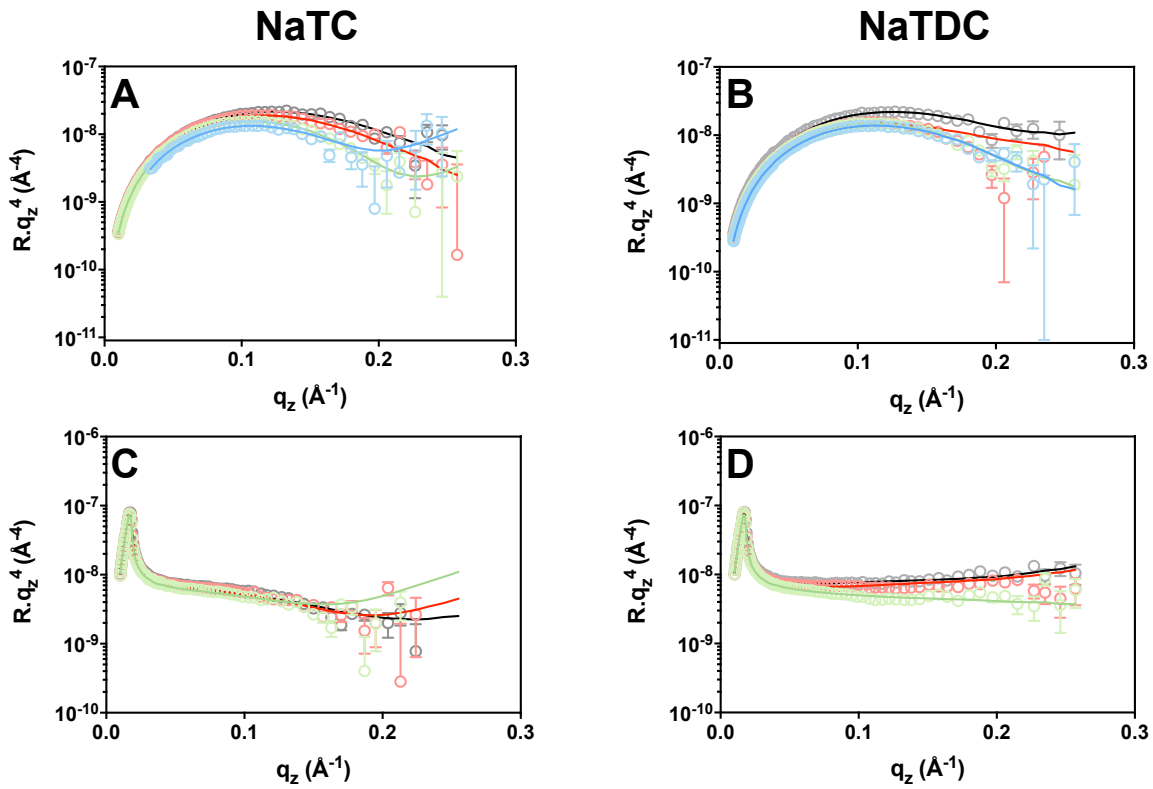

Figure S11: NR signal (*R.q*$_z^4$ representation) of the lipid monolayer as a function of the scattering vector (*q*$_z$) and its evolution upon successive injections of either NaTC (A, C) or NaTDC (B, D) into the aqueous subphase (at 23 ± 2°C). The lipids were spread onto water at π_{DPPC} = 25 ± 2 mN/m, thus forming a pure monolayer (○). BS concentrations below ((○) 1 mM), around ((○) 5 mM), and above ((○) 10 mM) their CMC were selected because different interfacial behaviours were observed with the LT. These NR data were recorded using ACMW, on which a monolayer of d_{75}-DPPC was prepared (A, B), and D_2O, on which a monolayer of either DPPC, for NaTC (C), or d_{75}-DPPC, for NaTDC (D), was prepared.

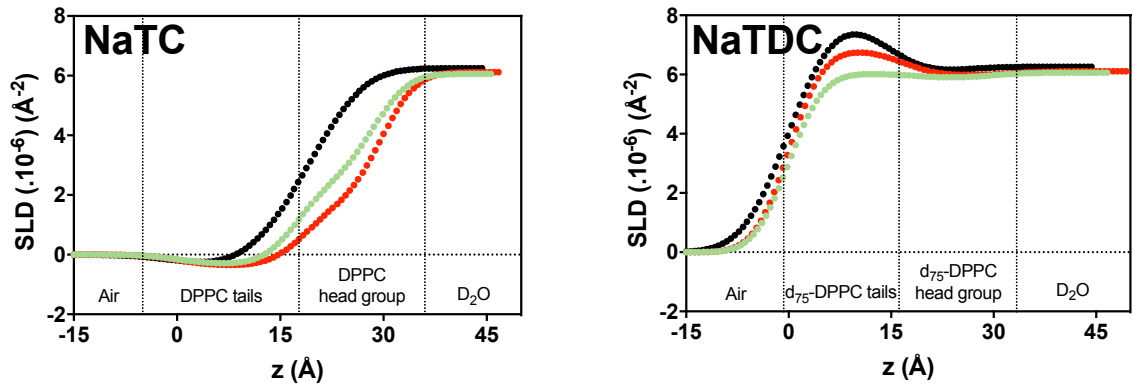

Figure S12: Evolution of the *SLD* profile of the interfacial film along the direction perpendicular to the surface (*z*) obtained from NR by successive injections of BS into the aqueous subphase: NaTC, NaTDC (at 23 ± 2°C). The lipids were spread onto water at π_{DPPC} = 25 ± 2 mN/m, thus forming a pure monolayer (●). These measurements were only performed at BS concentrations below ((●) 1 mM) and around ((●) 5 mM) their CMC. These *SLD* profiles were recorded in D_2O (*SLD* of 6.33×10^{-6} Å^{-2}), on which a monolayer of either DPPC (*SLD* of -0.41×10^{-6} Å^{-2} for the tails and 1.75×10^{-6} Å^{-2} for the head group), for NaTC (*SLD* of 0.95×10^{-6} Å^{-2}) (A), or d_{75}-DPPC (*SLD* of 7.66×10^{-6} Å^{-2} for the tails and 5.68×10^{-6} Å^{-2} for the head group), for NaTDC (*SLD* of 0.90×10^{-6} Å^{-2}) (B), was prepared.

NaTC		d_{75}-DPPC	[NaTC] (mM)			DPPC	[NaTC] (mM)	
			1	5	10		1	5
	σ (Å)	5	4	4	4	5	4	4
Tails	t (Å)	14	18	17	17	14	18	17
	SLD (×10^6) (Å^{-2})	8.1	6.9	5.9	5.3	-0.4	-0.4	-0.3
	f_{water}	0	0	0	0	0	0	0
Head group	t (Å)	7	11	11	11	7	11	11
	SLD (×10^6) (Å^{-2})	5.7	2.2	4.0	4.0	1.7	1.7	2.5
	f_{water}	0.1	0	0	0	0.1	0	0

NaTDC		d_{75}-DPPC	[NaTDC] (mM)		
			1	5	10
	σ (Å)	5	4	4	4
Tails	t (Å)	14	17	18	18
	SLD (×10^6) (Å^{-2})	8.1	6.8	6.0	5.8
	f_{water}	0	0	0	0
Head group	t (Å)	7	16	11	11
	SLD (×10^6) (Å^{-2})	5.7	5.7	5.7	2.3
	f_{water}	0.1	0.7	0.5	0

Table S2: Evolution of the NR parameters of each layer (tails and head group) of the lipid (either DPPC or d_{75}-DPPC) film: *σ*, the roughness, *t*, the thickness, *SLD*, the scattering length density and f_{water}, the amount of water, upon successive injections of 1, 5 and 10 mM BS into the aqueous subphase: NaTC, NaTDC.

Method of determination of the proportion of each component in each lipid film layer:

The proportion of each component (air, water, DPPC or BS) in each layer (lipid tails or head group) was determined using the following equation:

$$SLD_{layer} = \sum_i f_i \,.\, SLD_i \quad \text{(S1)}$$

where *i* represents each component present in the corresponding layer, SLD_{layer} the *SLD* of the corresponding layer fitted by the software, f_i and SLD_i, respectively, the proportion and *SLD* of the component *i* in the corresponding layer.

In the case of our study, and based on our assumptions (i.e., only air goes into the tails region, only water and BS go into the head group region), the *SLD* of the tails and head group layers are described as follows:

$$SLD_{tails\ layer} = f_{air} \,.\, \mathrm{SLD_{air}} + f_{tails} \,.\, \mathrm{SLD_{tails}} = f_{tails} \,.\, \mathrm{SLD_{tails}}, \text{ given that } \mathrm{SLD_{air}} = 0 \quad \text{(S2)}$$

$$SLD_{head\ group\ layer} = f_{water} \cdot \mathrm{SLD_{water}} + f_{BS} \cdot \mathrm{SLD_{BS}} + f_{head\ group} \cdot \mathrm{SLD_{head\ group}} \quad \text{(S3)}$$

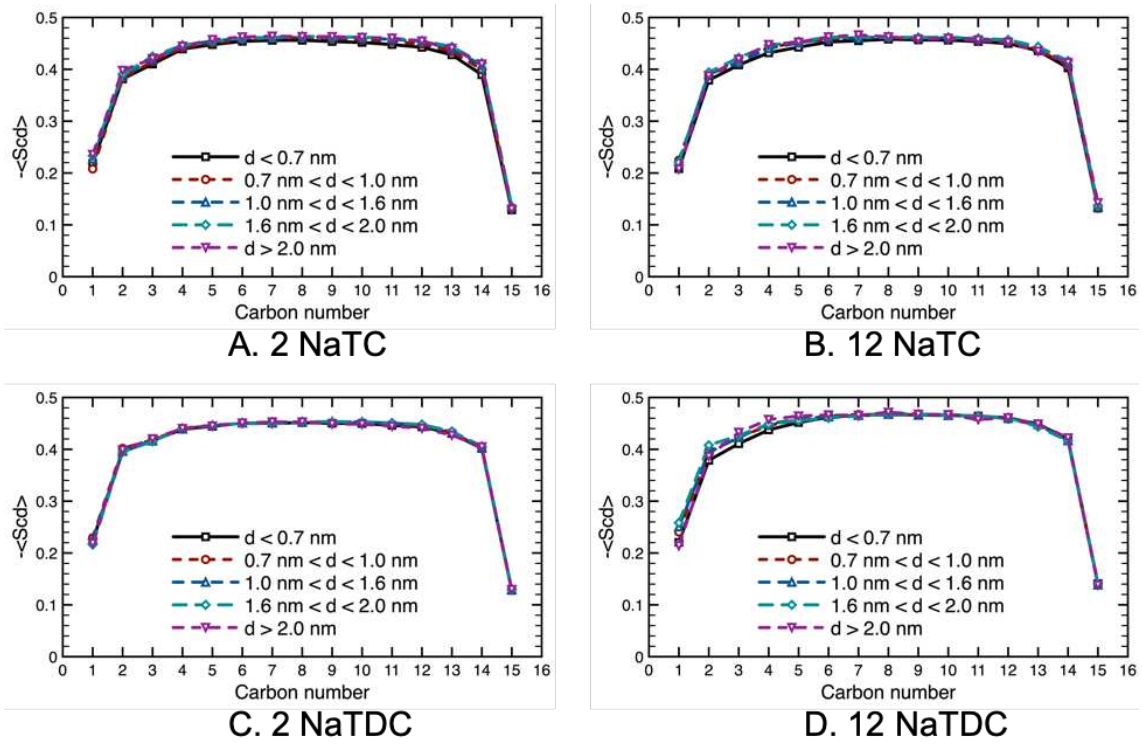

Figure S13: Average lipid order parameter of the *sn*-1 tail as a function of the depth in the DPPC monolayer, for different distances from a bound BS molecule in the presence of 2 (A, C) and 12 (B, D) molecules of BS: (A, B) NaTC, (C, D) NaTDC.

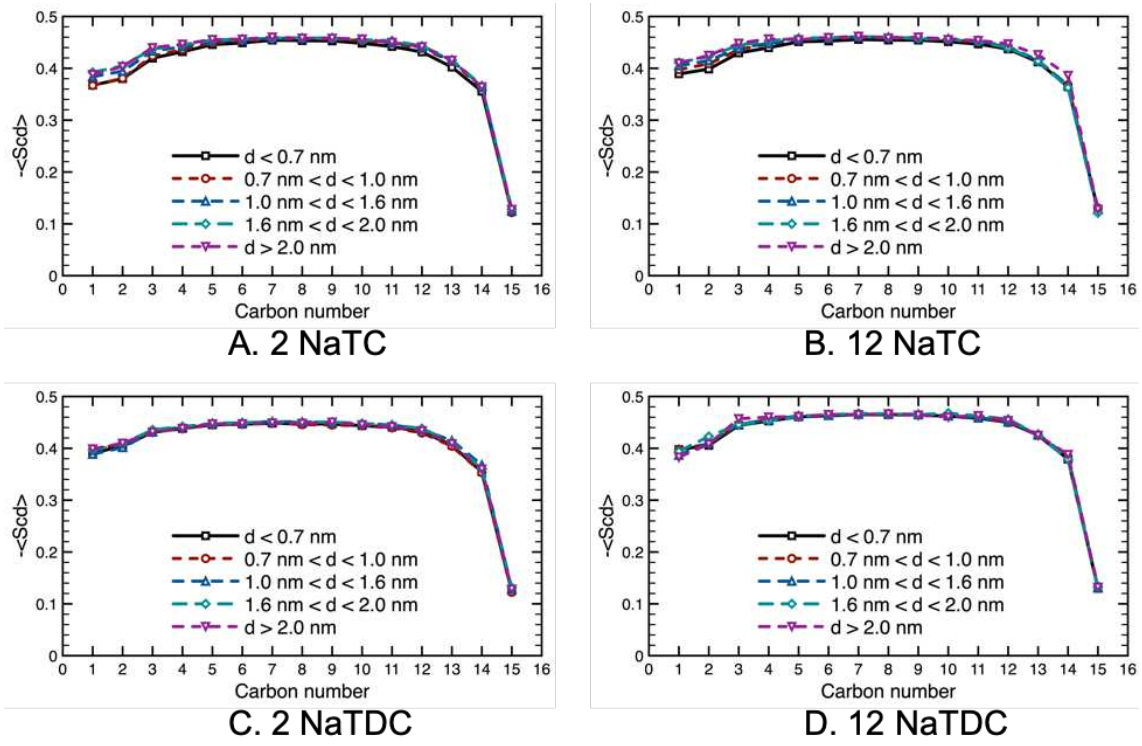

Figure S14. Average lipid order parameter of the *sn*-2 tail as a function of the depth in the DPPC monolayer, for different distances from a bound BS molecule in the presence of 2 (A, C) and 12 (B, D) molecules of BS: (A, B) NaTC, (C, D) NaTDC.

In each system, we have investigated the lipid order parameter of each lipid tail and then grouped them according to the distance that the lipid is from a bound BS molecule. We have plotted the lipid parameters as a function of the carbon number in the *sn*-1 (Figure S13) and *sn*-2 (Figure S14) tails in each system. As can be seen, there is very little effect on the order of the monolayers caused by the bound BS, independent of which type of BS is studied. If there is any difference at all, it is a very slight disordering of the lipid film near the ester group of the lipids (carbons 1 and 2) at small distances from the BS molecule.

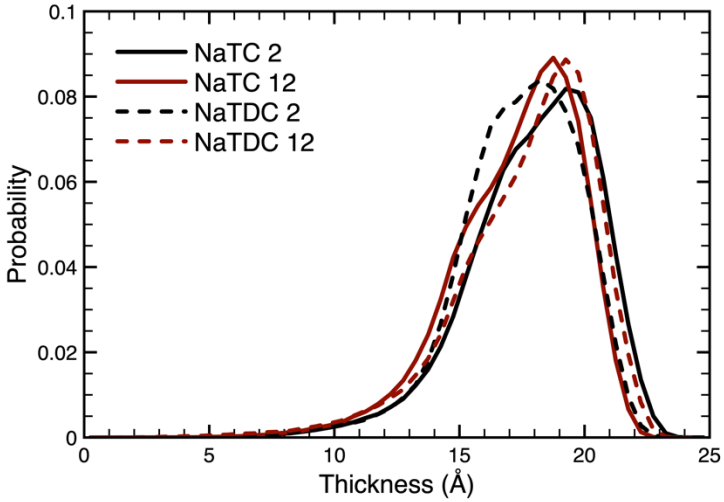

Figure S15: Distributions of the monolayer thickness for each of the four simulated systems: NaTC (━), NaTDC (- - -), with 2 (black) and 12 (red) BS.

We have also investigated the thickness of the monolayers in the systems we have simulated. Once again, we see very little difference in the thickness of the monolayers whether there are 2 or 12 BS molecules interacting with the monolayers (Figure S15).